Mineralogy and Petrology
https://doi.org/10.1007/s00710-022-00807-w

RESEARCH

Crystal structure and optical absorption spectra of $LiCo(SO_4)OH$ and its remarkable relationship to the Zn-Mn-silicate hodgkinsonite

Manfred Wildner[1] · **Gerald Giester**[1]

Received: 28 September 2022 / Accepted: 13 December 2022

Abstract

Crystals of the compound $LiCo(SO_4)OH$ were synthesised at low-hydrothermal conditions, and the crystal structure was determined and refined from single crystal X-ray diffraction data. $LiCo(SO_4)OH$ crystallises monoclinic, space group $P2_1/c$, $Z=4$, $a=9.586(2)$, $b=5.425(1)$, $c=7.317(1)$ Å, $\beta=109.65(1)°$, $V=358.3$ Å^3, $wR2=0.0485$ (2215 unique reflections, 78 variables). The structure is built from chains of edge-sharing, quite strongly bond-length and -angle distorted $Co(OH)_3O_3$ octahedra ($<Co–O>=2.126$ Å), which are further linked by common corners, hydrogen bonds, and by properly shaped SO_4 tetrahedra ($<S–O>=1.476$ Å) to sheets parallel (100). These sheets are connected to a three-dimensional framework by sharing corners with distorted LiO_4 polyhedra ($<Li–O>=1.956$ Å). Apart from the isotypic sulfates of Mn^{2+} and Fe^{2+}, only the molybdate $LiCd(MoO_4)OH$ crystallises isostructural with $LiCo(SO_4)OH$. However, a very close structural relationship exists with the rare mineral hodgkinsonite, $Zn_2Mn(SiO_4)(OH)_2$, yielding crystal chemically very uncommon topological equivalents of $Zn^{2+} \equiv S^{6+}$ and $Si^{4+} \equiv Li^+$, aside from the expectable substitution $Mn^{2+} \equiv Co^{2+}$. Polarised optical absorption spectra of $LiCo(SO_4)OH$ reveal that the dominating spin-allowed $^4T_1(P)$ band system of Co^{2+} (d^7 configuration) is strongly split up and covers a prominent part (~ 15,500–24,500 cm^{-1}) of the visible spectral range, in accordance with the significant distortion of the $Co(OH)_3O_3$ polyhedron. The spectra are interpreted in terms of the Superposition Model of crystal fields, yielding a new set of intrinsic and interelectronic repulsion parameters for Co^{2+}.

Keywords $LiCo(SO_4)OH$ · Crystal structure · Crystal chemistry · Optical absorption spectra · Superposition Model of crystal fields · Hodgkinsonite

Introduction

The crystal chemistry and spectroscopy of minerals and synthetic compounds with first-row transition metal cations in oxysalts of S, Se, or Te are long-lasting research topics at the authors' home institution, whereby well-defined synthetic phases can serve as model substances for the study of specific properties. In this respect, the new monoclinic compound $LiCo(SO_4)OH$ (space group $P2_1/c$ with $b<c<a$), prepared at low-hydrothermal conditions, provides several remarkable features (for a previous short note see Wildner et al. 2013a). Despite its rather simple composition, only very few isotypic compounds are known so far: These are, firstly, the respective compounds of Mn and Fe which have been studied together with the Co phase by powder diffraction techniques (Subban et al. 2013), $LiFe(SO_4)OH$ furthermore also by first principles calculations on the basis of density-functional theory (DFT) (Reshak and Khan 2014). The only other structurally characterised isotypic compound to date seems to be the molybdate $LiCd(MoO_4)OH$ (Kobtsev et al. 1968; Li and H atoms were not located directly); here, it has to be noted that the original description (Kobtsev et al. 1968) assigns it to space group $P2_1/a$ (correspondingly with $b<a<c$), but the given atomic coordinates obviously comply with cell setting $P2_1/c$. From a crystal chemical point of view, however, the close structural relationship of the title compound with hodgkinsonite, $Zn_2Mn(SiO_4)(OH)_2$ ($P2_1/a$, $b<a<c$; Rentzeperis 1963), a rare mineral found at the Franklin mine, New Jersey, USA, is even more remarkable, since it exemplifies the possibilities of some crystal chemically very uncommon topological equivalents.

Editorial handling: T. Armbruster

✉ Manfred Wildner
manfred.wildner@univie.ac.at

[1] Institut für Mineralogie und Kristallographie, Universität Wien, Josef-Holaubek-Platz 2, 1090 Vienna, Austria

Published online: 04 January 2023

The crystal structure of $LiCo(SO_4)OH$ features rather strongly distorted $Co(OH)_3O_3$ octahedra with bond lengths and *cis*-angles ranging between 2.04 to 2.22 Å and 80.1 to 104.5°, respectively. The distortion makes $LiCo(SO_4)OH$ an ideal candidate for the resolution of low-symmetry crystal field (CF) splittings of *d-d* electronic transitions of $3d^7$-configurated Co^{2+}. In turn, this may allow to derive a reliable set of crystal field parameters (CFPs) for Co^{2+} in terms of the semiempirical Superposition Model of crystal fields (SPM), originally mainly applied to *f*-element systems (Newman 1971; Newman and Ng 1989, 2000), but increasingly also adopted for *d*-block cations (see, e.g., Andrut et al. 2004, or the recent review with extensive database by Rudowicz et al. 2019).

Experimental

Synthesis

Crystals of the new compound $LiCo(SO_4)OH$ were synthesized at low-hydrothermal conditions in Teflon-lined steel autoclaves (~5 cm^3 reaction volume, 10 days at 210 °C). A stoichiometric mixture of $Co(OH)_2$ and Li_2CO_3, dissolved in access of concentrated H_2SO_4, plus H_2O were used as starting materials. The filling level of the reaction chamber was ≤25%. Reddish-pink, rhombus-shaped platy crystals up to 0.5 mm were obtained.

Single-crystal X-ray diffraction

The structure investigation was performed at room temperature on a Bruker-Nonius APEXII diffractometer equipped with a monocapillary optics collimator (graphite monochromatized Mo *K*α radiation). Data were measured up to 80° 2θ full sphere (phi and omega scans, 2° scan width) at a crystal-detector distance of 35 mm. Absorption was corrected by evaluation of multi-scans. The structure was solved in space group $P2_1/c$ by direct methods and refined by full-matrix least-squares techniques on F^2 with the programs SHELXS and SHELXL, respectively (Sheldrick 2008, 2015). Oxygen atoms were labelled according to the isotypic structure of $LiCd(MoO_4)OH$ with 'O5' changed to 'Oh' (Kobtsev et al. 1968; for details see the "Introduction" section). However, their specific atomic coordinates were selected to form direct bonds to S (O1 to O4) and Co (one Oh), respectively, and for all atoms to lie within the unit cell. Anisotropic displacement parameters (ADP) for all non-hydrogen atoms were applied. Information on crystal data, procedures of measurements and refinements are compiled in Table 1, final atomic parameters are listed in Table 2. Further details of the crystal structure investigation of $LiCo(SO_4)OH$ may be obtained from the joint CCDC/FIZ Karlsruhe online deposition service: https://www.ccdc.cam.ac.uk/structures/? by quoting the deposition number CSD 2215181.

Table 1 Crystal data and details of the intensity measurement and structure refinement for $LiCo(SO_4)OH$

Crystal Data	$LiCo(SO_4)OH$
Space group	$P2_1/c$
a (Å)	9.586(2)
b (Å)	5.425(1)
c (Å)	7.317(1)
β (°)	109.65(1)
V (Å^3)	358.3(1)
Z	4
ρ_{calc} (g cm^{-3})	3.317
μ (Mo*K*α) (mm^{-1})	5.25
Data collection and refinement	
Unique data	2215
Data with $F_o > 4\sigma(F_o)$	1797
Variables	78
*R*1 [for $F_o > 4\sigma(F_o)$][1]	0.0257
*wR*2 [for all F_o^2][1]	0.0485
a, b[1]	0.012, 0.3
$\Delta\rho_{min\,/\,max}$ (eÅ^{-3})	-0.68 / 0.62

[1] $R1 = \Sigma\ F_o - F_c\ /\ \Sigma\ F_o$; $wR2 = [\Sigma w(F_o^2 - F_c^2)^2\ /\ \Sigma w(F_o^2)^2]^{½}$; $w = 1\ /\ [\sigma^2(F_o^2) + (a \times P)^2 + b \times P]$; $P = \{[\text{max of } (0 \text{ or } F_o^2)] + 2F_c^2\}\ /\ 3$

Polarised optical absorption spectroscopy

Polarised optical absorption spectra of $LiCo(SO_4)OH$ in the spectral range 34,000–5000 cm^{-1}, i.e. covering the near ultraviolet (UV), the visible (Vis) and the near-infrared (NIR) range of the electromagnetic spectrum, were measured on (100) plates parallel to the *b*- and *c*-axes, and on a platy [~$(20\bar{5})$] crystal fragment parallel to a^*-axis, using a mirror-optics microscope IR-scopeII, attached to a Bruker IFS66v/S FTIR spectrometer. A quartz beam splitter, a calcite Glan-prism polariser, and appropriate combinations of light sources (Xenon or Tungsten lamp) and detectors (GaP-, Si- or Ge-diodes) were used to cover the desired spectral range, using measuring spots between 100 and 165 µm in diameter. Hence, each full spectrum is combined from three partial spectra (34,000–20,500 cm^{-1}: spectral resolution 40 cm^{-1}, averaged from 1024 scans; 20,500–10,000 and 10,000–5000 cm^{-1}: spectral resolution 20 cm^{-1}, averaged from 512 and 256 scans, respectively), which were aligned in absorbance for perfect match, if necessary, and calculated to linear absorption coefficient α (cm^{-1}). The transition energies observed in the optical spectra were extracted by visual inspection and subsequently used in the CF calculations.

Table 2 Atomic coordinates and displacement parameters for $LiCo(SO_4)OH$ with e.s.d.'s in parentheses. The ADP are defined as $exp(-2\pi^2\sum_i\sum_j U_{ij}h_ih_j a_i^* a_j^*)$, the U_{eq} as $\frac{1}{3}\sum_i\sum_j U_{ij}\, a_i^* a_j^*\, \mathbf{a}_i.\mathbf{a}_j$ (Fischer and Tillmanns 1988)

	x	*y*	*z*	$U_{iso/eq}$	U^{11}	U^{22}	U^{33}	U^{23}	U^{13}	U^{12}
Co	0.44622(2)	0.23532(2)	0.37825(2)	0.00724(2)	0.00847(4)	0.00670(5)	0.00670(4)	0.00047(4)	0.00275(3)	0.00018(4)
S	0.21027(2)	0.56073(4)	0.51324(3)	0.00647(4)	0.00582(6)	0.00645(8)	0.00691(7)	0.00024(6)	0.00183(5)	0.00036(6)
Li	0.0785(2)	0.0654(4)	0.3202(3)	0.0167(4)	0.0178(8)	0.0133(8)	0.0165(8)	0.0010(7)	0.0023(6)	-0.0013(7)
O1	0.09572(7)	0.41817(14)	0.36722(10)	0.01139(13)	0.0085(2)	0.0115(3)	0.0123(3)	-0.0033(2)	0.00088(19)	-0.0018(2)
O2	0.16059(8)	0.81537(13)	0.51690(10)	0.01126(13)	0.0125(3)	0.0079(3)	0.0137(3)	0.0005(2)	0.0048(2)	0.0022(2)
O3	0.24058(7)	0.44551(14)	0.70535(9)	0.01161(13)	0.0116(2)	0.0149(3)	0.0091(2)	0.0045(2)	0.00448(18)	0.0036(2)
O4	0.34956(7)	0.55723(13)	0.46388(9)	0.00896(12)	0.0070(2)	0.0102(3)	0.0104(2)	-0.0003(2)	0.00391(17)	-0.0003(2)
Oh	0.43352(7)	0.07246(13)	0.63206(9)	0.00825(12)	0.0091(2)	0.0078(3)	0.0083(2)	-0.0004(2)	0.00340(17)	-0.0003(2)
H	0.3478(16)	0.020(3)	0.605(2)	0.021(4)						

The superposition model of crystal fields – background theory and calculations for $LiCo(SO_4)OH$

Crystal field calculations were performed in the framework of the semiempirical Superposition Model of crystal fields, originally developed by Newman (1971) to separate the geometrical and physical information contained in crystal field parameters, taking into account the exact geometry of the coordination polyhedra in the respective phases. The SPM is based on the assumption that the CF can be expressed as the sum of axially symmetric contributions of all *i* nearest neighbour ligands of the transition metal cation. The CFPs B_{kq} in Wybourne notation are then obtained from

$$B_{kq} = \sum_i \overline{B}_k(R_0)\left(\frac{R_0}{R_i}\right)^{t_k} K_{kq}(\Theta_i, \Phi_i),$$

where $\overline{B}_k$ are the 'intrinsic' parameters (related to a reference metal–ligand distance R_0), t_k are the power-law exponent parameters, both for each rank k of the CFPs, R_i are the individual metal–ligand distances, and $K_{kq}(\Theta_i,\Phi_i)$ are the coordination factors calculated from the angular polar coordinates of the ligands. For details and comprehensive reviews on the SPM refer to Newman (1971), Newman and Ng (1989, 2000), Rudowicz et al. (2019), and (with geoscientific focus) Andrut et al. (2004); for a review on the explicit forms of low-symmetry CF Hamiltonians the reader is referred to Rudowicz et al. (2011).

The actual CF calculations were done using the HCFLDN2 module of the computer program by Yau-yuen Yeung (Rudowicz et al. 1992; Chang et al. 1994; Yang et al. 2004), which includes imaginary CF terms and is thus applicable to arbitrary low symmetries of all $3d^N$ electron systems. A suite of supplementary programs (Manfred Wildner, unpublished) was used to manage the input and output of the HCFLDN2 program, in particular (i) for the transformation of atomic to polyhedral polar coordinates; (ii) for the systematic variation of intrinsic and power-law SPM parameters, as well as of the Racah parameters B and C; (iii) for the SPM calculation itself, giving the actual values of the CFPs B_{kq}'s; (iv) for the corresponding communication with a slightly modified version of the HCFLDN2 program (Yau-yuen Yeung, personal communication); and (v) for the interpretation and evaluation of the HCFLDN2 output results in terms of a reliability index for the agreement of calculated and observed transition energies.

In the case of the triclinic point symmetry group 1 (C_1) of the $Co(OH)_3O_3$ polyhedron in $LiCo(SO_4)OH$, symmetrically unrestricted SPM calculations including all 14 B_{kq} CFPs (with rank $k=2$ and 4) were performed; however, to reduce the number of variables (accompanied by reduced CPU time) and to improve the transferability of intrinsic $\overline{B}_k$ parameters, the power-law exponent parameters t_k were fixed at their ideal electrostatic values of $t_4=5$ and $t_2=3$. The reference metal–ligand distance R_0 for Co^{2+} was set to 2.1115 Å, i.e. the overall mean Co–O bond length in six-fold coordination (Wildner 1992). For comparison with classical CFPs, a Dq_{cub} value (representing the strength of CF acting on a metal ion within an ideal octahedron) was calculated from the B_{kq}'s via the rotational invariant s_4 (Leavitt 1982), i.e. $Dq_{cub}=s_4/(2\sqrt{21})$. Note that the intrinsic $\overline{B}_k$ parameters (and if refined also the power-law exponents t_k) can be directly compared with the results of SPM analyses carried out by others. However, the comparison of SPM calculations of orthorhombic, monoclinic, and triclinic B_{kq} CFPs with respective sets from other sources would require rotations to obtain the standardized parameter sets (see, e.g. Newman and Ng 2000; Rudowicz and Jian 2002; Gnutek and Rudowicz 2008, and references in these papers). The pertinent standardization calculations for Co^{2+} ions in $LiCo(SO_4)OH$ are, however, beyond the scope of the present study.

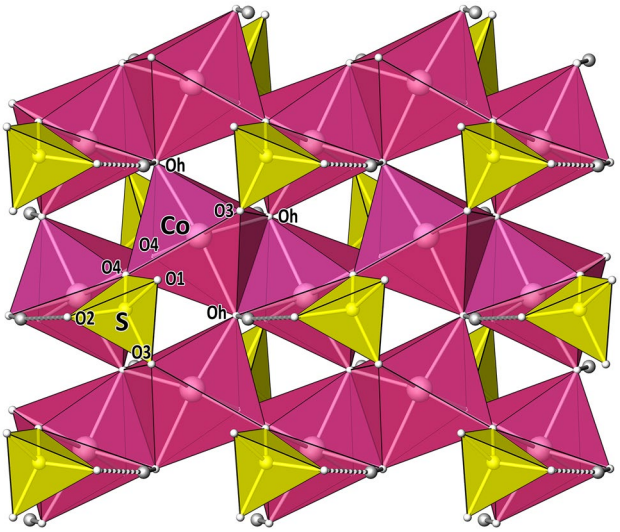

Fig. 1 Sheet of $Co(OH)_3O_3$ octahedra with adjacent SO_4 tetrahedra in the crystal structure of $LiCo(SO_4)OH$ in a projection on (100)

Results and discussion

Crystal structure description

The crystal structure of $LiCo(SO_4)OH$ is built from chains of edge-sharing $Co(OH)_3O_3$ polyhedra which are linked by sharing corners among each other and with SO_4 tetrahedra to sheets parallel (100) (Fig. 1). These sheets are further connected to a three-dimensional structure by sharing corners with LiO_4 polyhedra (Fig. 2a). The oxygen atom (Oh) which is shared by three CoO_6 polyhedra acts as donor of a hydroxyl group, while the oxygen atom linking one S and one Li atom (O2) is acceptor of a moderately strong, intra-sheet hydrogen bond (Oh···O2 = 2.831 Å), in agreement with its slightly reduced bond valence sum (1.82 v.u. in Table 3). All atoms are located on general positions and each cation forms one crystallographically distinct type of polyhedron. Selected crystal chemical data and bond valences are compiled in Table 3.

The CoO_6 polyhedron (Fig. 3) exhibits considerable distortion with three shorter Co–O bonds to OH groups (Co–Oh = 2.045 – 2.097 Å) and three longer bonds to oxygen atoms of SO_4 tetrahedra (Co–O = 2.166 – 2.216 Å). *Cis*-bond angles range from 80.1 – 104.5°; the two longest bonds are *trans*-located, thus forming a roughly pseudo-tetragonally elongated octahedron. The extents of the octahedral bond length and especially bond angle distortion (Table 3) per se are not unusual for CoO_6 polyhedra (Wildner 1992), but both combined in one polyhedron are less common. The mean Co–O bond length of 2.126 Å is above average (2.1115 Å; Wildner 1992), thus complying with the distortion theorem by Brown and Shannon (1973). Similarly, the LiO_4 polyhedron is strongly distorted (Table 3), especially concerning its angular and related edge-length distortion; in fact, it ranges among the strongest combined bond-length/edge-length distortions found for LiO_4 tetrahedra without shared edges, as compiled by Wenger and Armbruster (1991). In contrast, the sulfate tetrahedron adopts a much more regular shape, especially in terms of its small angular distortion.

A comparison of $LiCo(SO_4)OH$ with the structures of $LiM(SO_4)OH$ (M^{2+} = Mn, Fe, Co) obtained from powder diffraction

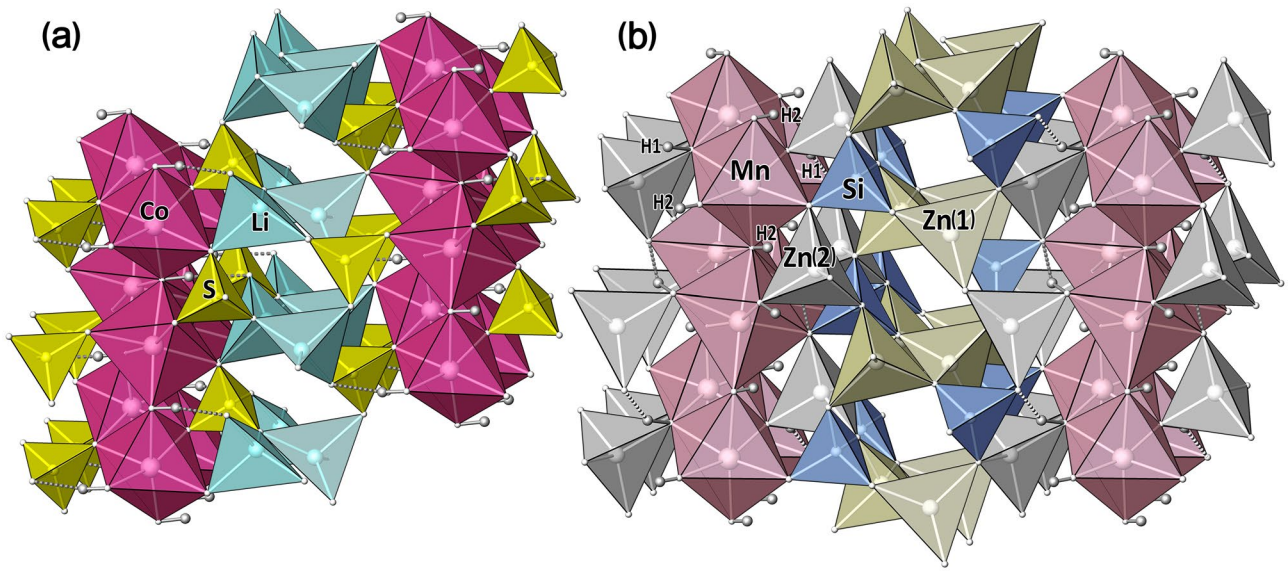

Fig. 2 Crystal structures of **(a)** $LiCo(SO_4)OH$ and **(b)** hodgkinsonite, $Zn_2Mn(SiO_4)(OH)_2$ (Rentzeperis 1963), in projections approximately along [010]. Comparison of **(a)** and **(b)** reveals uncommon topological equivalences of SO_4 with ZnO_4 tetrahedra and LiO_4 with SiO_4 tetrahedra in $LiCo(SO_4)OH$ and $Zn_2Mn(SiO_4)(OH)_2$, respectively

Table 3 Selected interatomic bond lengths (Å), angles or angular ranges (°), bond strengths ν (v.u.; calculated – without H atoms – according to Brese and O'Keeffe 1991), and polyhedral distortion parameters (Δ_{oct}: Brown and Shannon 1973; σ_{oct}^2 and σ_{tetr}^2: Robinson et al. 1971; BLDP and ELDP: Griffen and Ribbe 1979; BLD and ELD: Renner and Lehmann 1986) in $LiCo(SO_4)OH$

Co–Oh	2.0448(7)	S–O2	1.4644(8)
–Oh′	2.0493(7)	S–O1	1.4684(7)
–Oh″	2.0967(7)	S–O3	1.4752(7)
–O4	2.1660(8)	S–O4	1.4960(8)
–O3	2.1843(7)	<S–O>	1.476
–O4′	2.2163(7)	$\Sigma\nu_{S-O}$	5.97
<Co–O>	2.126	BLDP × 10^3	9.53
$\Sigma\nu_{Co-O}$	1.89		
$\Delta_{oct} \times 10^3$	0.98	O–S–O_{min}	108.59(4)
		O–S–O_{max}	110.08(4)
Oh–Co–Oh′	104.52(2)	σ_{tetr}^2	0.34
–Oh″	83.68(2)		
–O4	166.02(2)		
–O3	91.26(3)	Li–O1	1.941(2)
–O4′	91.36(3)	Li–O2	1.941(2)
Oh′–Co–Oh″	171.49(3)	Li–O1′	1.942(2)
–O4	86.52(3)	Li–O3	2.001(2)
–O3	86.80(3)	<Li–O>	1.956
–O4′	88.89(3)	$\Sigma\nu_{Li-O}$	1.07
Oh″–Co–O4	85.74(3)	BLDP × 10^3	15.16
–O3	90.79(3)	BLD	1.14
–O4′	93.25(3)		
O4–Co–O3	98.00(3)	O1–Li–O2	105.91(10)
–O4′	80.13(3)	–O1′	122.18(10)
O3–Co–O4′	175.40(3)	–O3	107.23(10)
σ_{oct}^2	42.06	O2–Li–O1′	124.63(10)
		–O3	96.44(9)
		O1′–Li–O3	94.12(9)
		σ_{tetr}^2	161.57
		ELDP × 10^3	72.50
		ELD	5.73
$\Sigma\nu_{O1}$	2.08		
$\Sigma\nu_{O2}$	1.82	Oh–H	0.829(15)
$\Sigma\nu_{O3}$	2.00	H···O2	2.022(15)
$\Sigma\nu_{O4}$	1.93	Oh···O2	2.8315(11)
$\Sigma\nu_{Oh}$	1.10	Oh–H···O2	165.3(15)

data (Subban et al. 2013), and in case of the Fe-compound also by DFT calculations (Reshak and Khan 2014), shows a basic agreement, e.g. in that the three shorter octahedral bonds are formed with the OH groups, but an advanced analysis is hardly useful considering the inherent deficiencies in the powder (and DFT) data vs. the present single crystal data. In isotypic $LiCd(MoO_4)OH$ (Kobtsev et al. 1968) the Li and H atoms could not be located, but a (topologically basically correct) position for Li was postulated. Anyway, the Li-polyhedra in both compounds

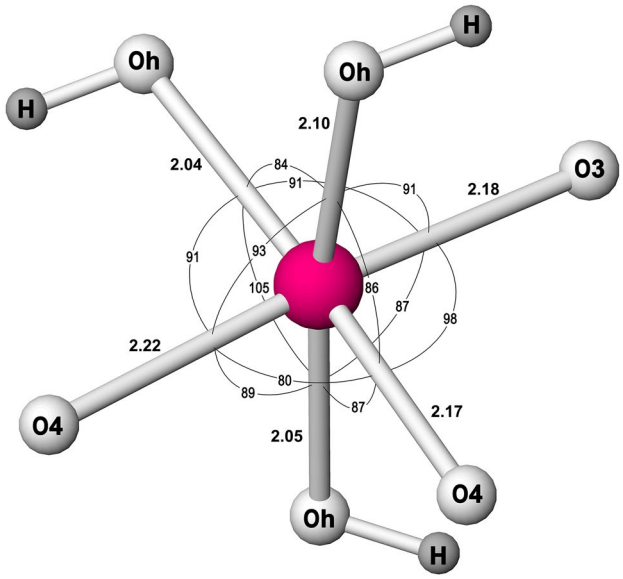

Fig. 3 Geometry of the $Co(OH)_3O_3$ polyhedron in $LiCo(SO_4)OH$ with rounded Co–O bond lengths (Å) and *cis* bond angles (°)

can hardly be compared (e.g., Kobtsev et al. 1968 claim Li–O distances of 1.92 – 2.07 Å, but a recalculation in the corrected setting – see Introduction – gives 1.57 Å as lower limit). Also the fundamental differences of respective central atoms in the $M^{2+}O_6$ and $X^{6+}O_4$ polyhedra prevent a useful comparison; e.g., the MoO_4 group is strongly distorted compared to the quite regular SO_4 tetrahedron in the title compound.

Anyway, Kobtsev et al. (1968) pointed out that $LiCd(MoO_4)OH$ – and hence also $LiCo(SO_4)OH$ – is structurally related to the rare mineral hodgkinsonite, $Zn_2Mn(SiO_4)(OH)_2$ (Rentzeperis 1963). The structure of hodgkinsonite (a=8.171 Å, b=5.316 Å, c=11.761 Å, β=95.15°, V=508.7 Å^3, space group $P2_1/c$) shown in Fig. 2b contains octahedral-tetrahedral sheets which are topologically identical to those shown in Fig. 1 for $LiCo(SO_4)OH$, but composed of $MnO(OH)_5$ octahedra and $Zn(2)O_4$ tetrahedra. A comparison of Figs. 2a and b reveals that in hodgkinsonite the roles of the inter-sheet-linking LiO_4 tetrahedra in $LiCo(SO_4)OH$ are somewhat surprisingly taken by SiO_4 tetrahedra, as well as by a second type of ZnO_4 tetrahedra, i.e. $Zn(1)O_4$, without topological equivalence in $LiCo(SO_4)OH$. These $Zn(1)O_4$ tetrahedra are inserted between adjacent sheets in hodgkinsonite and form their sole direct linkage. Hence, perpendicular to the structural sheets the lattice expands at a higher rate than caused solely by the larger ionic radii of Mn and Si in hodgkinsonite relative to Co and S, respectively, in $LiCo(SO_4)OH$ (radius $Zn^{2+} \approx Li^+$), and the cell angle β is reduced by nearly 14°. The layout of the hydrogen bonding scheme in hodgkinsonite is not as clear-cut as in $LiCo(SO_4)OH$. The $MnO(OH)_5$ octahedron includes two crystallographically different donor oxygen atoms of hydroxyl groups. According to Rentzeperis (1963), one of them (O6–H2 ≡ Oh–H···O2 in the title compound) forms no hydrogen bond (the

corresponding bridge O6···O1 = 3.10 Å with already overbonded O1); the other one (O5–H1 ≡ the 'plain' O4 in the title compound) forms a weak intra-sheet hydrogen bond in hodgkinsonite (to O2 ≡ O3; a recalculation of bond valences from the structure data of Rentzeperis 1963 also supports this assignment). Irrespective of any uncertainties regarding possible hydrogen bond acceptor oxygens, the formation of inter-sheet hydrogen bonds can be excluded.

Polarised optical absorption spectra and crystal field calculations

The strong and irregular bond-length and -angle distortion of the CoO_6 polyhedron with point symmetry group 1 (C_1) (Fig. 3) makes $LiCo(SO_4)OH$ a promising candidate for the resolution of low-symmetry absorption band splittings of the generally broad spin-allowed absorption bands of Co^{2+} with cubic quartet ground state $^4T_1(F)$. In fact, as evident in Fig. 4, the intense spin-allowed $^4T_1(P)$ band system is strongly split up and covers a prominent part (approx. 15,500 – 24,500 cm^{-1}) of the visible spectral range. In contrast, the weaker spin-allowed $^4T_2(F)$ band in the NIR region (centred around 7500 cm^{-1}) shows only weak splitting, and the spin-allowed but electronically forbidden $^4A_2(F)$ band (at ~ 14,800 cm^{-1}) does not split up since the $^4A_2(F)$ state is a non-degenerate orbital singlet. As a consequence of the strong splitting and broadening of the intense $^4T_1(P)$ state in $LiCo(SO_4)OH$, generally weak spin-forbidden doublet levels (arising from the doublet ^2G, ^2P and ^2H terms) are now located at the onset or within the $^4T_1(P)$ band system and can'steal' significant intensity (i.e. partly gain quartet character) from the spin-allowed bands due to spin–orbit coupling. In particular, sharp features assigned to the more or less field-independent levels $^2T_{1,2}(G)$ at 16,110 cm^{-1} and especially $^2T_1(P)$ at 19,990 and 20,540 cm^{-1} exhibit strong intensity stealing. Since for transition metal ions at triclinic symmetry sites – as Co^{2+} at point symmetry group 1 (C_1) in the present case – all CF levels split completely and hence their states become orbital singlets, which transform as A-states, and the above-mentioned vague pseudo-tetragonal elongation is not pronounced enough, a meaningful analysis of the polarisation behaviour is not feasible. At least it

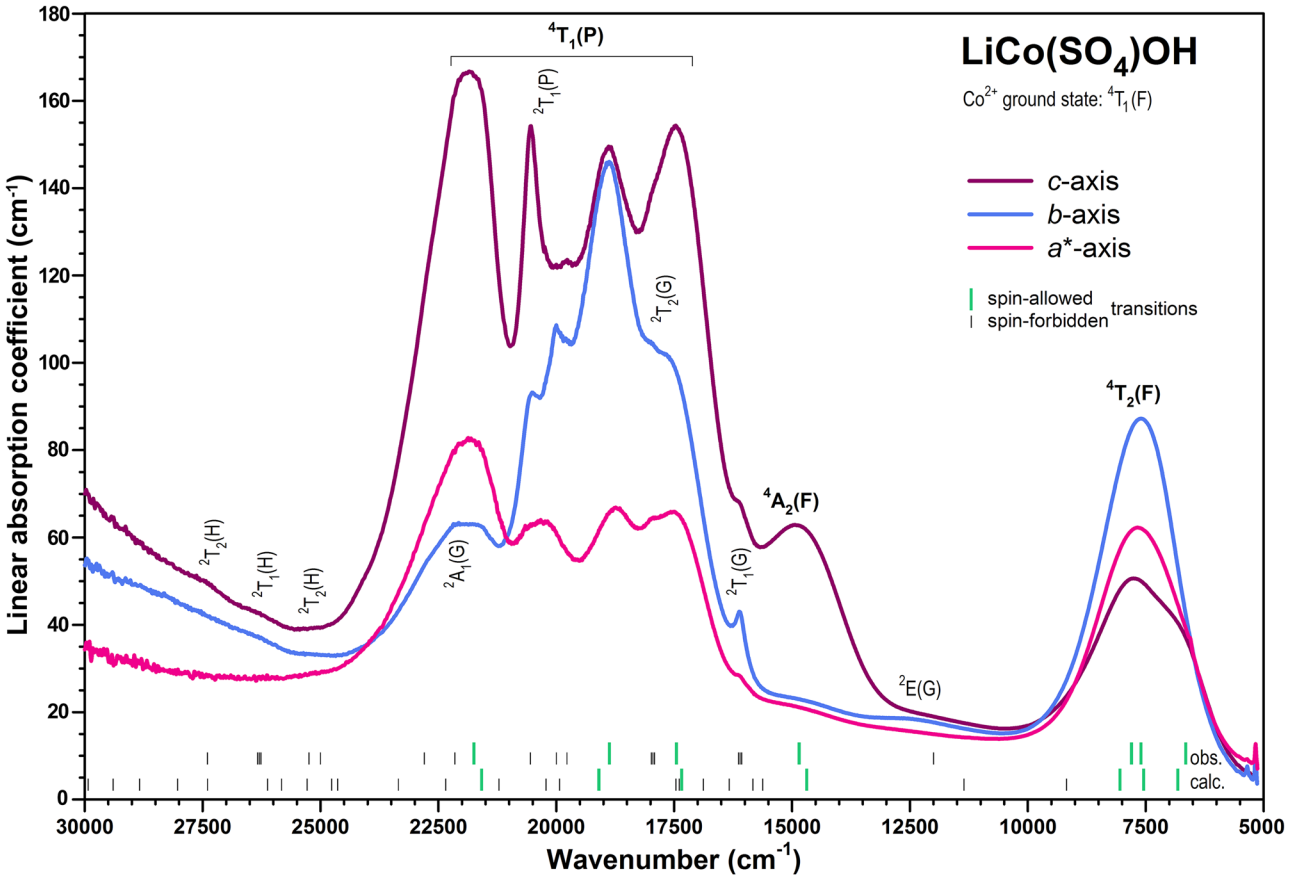

Fig. 4 Polarised optical absorption spectra of $LiCo(SO_4)OH$ with assignments of CF levels for cubic symmetry (spin-allowed states in bold, spin-forbidden in normal narrow letters). Tick marks indicate observed and calculated energy levels for triclinic symmetry

can be stated that the transition intensity seems to be enhanced when the electric vector lies within the octahedral sheet, i.e. parallel to the *b*- and *c*-axes (Fig. 4).

Results of the SPM calculations (for details see the section on background theory above) for $LiCo(SO_4)OH$ are listed in Table 4, and corresponding calculated energy levels are indicated in Fig. 4. Compared to previous SPM analyses of Co^{2+} compounds (see, e.g., Andrut et al. 2004; Brik and Yeung 2008), the order of the intrinsic parameters $\overline{B}_2 >> \overline{B}_4$ is rather surprising. Generally, $\overline{B}_2 >> \overline{B}_4$ is expected from theory (Newman and Ng 1989), but in case of $3d^N$ transition ions this sequence is often not observed, sometimes even $\overline{B}_2 < \overline{B}_4$ is found (Andrut et al. 2004; Wildner et al. 2013b), especially if spin-allowed and spin-forbidden levels are fitted to the same respective set of SPM parameters. In terms of classical CF and interelectronic repulsion parameters, the obtained parameters Racah B (815 cm^{-1}) and C as well as and the average CF strength parameter Dq_{cub} (786 cm^{-1}, calculated from the triclinic B_{kq}'s) fit well in the expected range for Co^{2+} in octahedral coordination in oxysalts (as compiled, e.g., by Wildner et al. 2004); only the ratio Racah C/B is somewhat above average. Overall, the remarkable magnitude of low-symmetry band splittings in the spectra of $LiCo(SO_4)OH$, especially of the $^4T_1(P)$ system, allows to extract well defined transition energies. Hence, the various spectroscopic parameters listed in Table 4 are assumed to be very reliable, and may thus serve as starting values in CF calculations of other Co^{2+}-bearing inorganic compounds.

Table 4 Summary of refined SPM (intrinsic $\overline{B}_k$) and interelectronic repulsion parameters (Racah B, C), as well as of calculated (real and imaginary B_{kq} CFPs in Wybourne notation and rotational invariants s_k), derived (cubic CF strength Dq_{cub} and 'covalency indicator' $\beta = B/B_0$), or fixed (power-law exponents t_k) parameters for Co^{2+} ions in $LiCo(SO_4)OH$

d electrons	7
Symmetry	1
R_0 (Å)	2.1115
B_{20} (cm^{-1})	–3661
B_{21} (cm^{-1})	4 + 2297 i
B_{22} (cm^{-1})	1324 – 3219 i
B_{40} (cm^{-1})	15,788
B_{41} (cm^{-1})	36 – 1077 i
B_{42} (cm^{-1})	–690 + 826 i
B_{43} (cm^{-1})	–30 – 1061 i
B_{44} (cm^{-1})	10,084 + 1877 i
$\overline{B}_4$ (cm^{-1})	5045
$\overline{B}_2$ (cm^{-1})	13,430
t_4 / t_2 (fixed)	5 / 3
s_4 (cm^{-1})	7200
s_2 (cm^{-1})	3105
Racah B (cm^{-1})	815
β ($B_0 = 989$ cm^{-1})	0.82
Racah C (cm^{-1})	3870
Racah C/B	4.75
Dq_{cub} (from s_4) (cm^{-1})	786

Conclusions

Despite its rather simple composition and well-defined crystal structure, the new synthetic compound $LiCo(SO_4)OH$ exhibits some remarkable chemical and spectroscopic features. While up to date only a very limited number of isotypic phases has been identified, $LiCo(SO_4)OH$ is closely related to the mineral hodgkinsonite, $Zn_2Mn(SiO_4)(OH)_2$, revealing surprising topological equivalences of tetrahedral $Zn^{2+} \equiv S^{6+}$ and $Si^{4+} \equiv Li^+$, as well as of octahedral $MnO(OH)_5 \equiv Co(OH)_3O_3$. The $Co(OH)_3O_3$ polyhedron shows strong combined bond-length and angular distortions, allowing to properly resolve low-symmetry absorption band splittings in the optical absorption spectra of LiCo(SO4)OH. This enables deriving reliable CF parameters as well as interelectronic repulsion ones for Co^{2+} ions in $LiCo(SO_4)OH$.

Supplementary Information The online version contains supplementary material available at https://doi.org/10.1007/s00710-022-00807-w.

Acknowledgements This work is dedicated to Prof. Dr. Josef Zemann on the occasion of his 100th birthday. Detailed reviews by Czeslaw Rudowicz and an anonymous expert helped to significantly improve the manuscript. Additional fruitful discussions with Czeslaw Rudowicz are highly appreciated. Thanks are also due to guest editor Thomas Armbruster for editorial handling of the manuscript.

Author contributions Both authors contributed equally to, and reviewed the manuscript.

Funding Open access funding provided by University of Vienna.

Declarations

Competing interests The authors declare no competing interests.

References

Andrut M, Wildner M, Rudowicz CZ (2004) Optical absorption spectroscopy in geosciences: Part II: Quantitative aspects of crystal fields. EMU Notes in Mineralogy 6:145–188

Brese NE, O'Keeffe M (1991) Bond-Valence Parameters for Solids Acta Cryst B47:192–197

Brik MG, Yeung YY (2008) Semi-ab initio calculations of superposition model and crystal field parameters for Co^{2+} ions using the exchange charge model. J Phys Chem Solids 69:2401–2410

Brown ID, Shannon RD (1973) Empirical bond-strength-bond-length curves for oxides. Acta Cryst A29:266–282

Chang YM, Rudowicz C, Yeung YY (1994) Crystal field analysis of the $3d^N$ ions at low symmetry sites including the "imaginary" terms. Computers Phys 8:583–588

Fischer RX, Tillmanns E (1988) The equivalent isotropic displacement factor. Acta Cryst C44:775–776

Gnutek P, Rudowicz C (2008) Diagonalization of second-rank crystal field terms for $3d^N$ and $4f^N$ ions at triclinic or monoclinic symmetry sites – case study: Cr^{4+} in Li_2MgSiO_4 and Nd^{3+} in β-BaB_2O_4. Optic Mater 31:391–400

Griffen DT, Ribbe PH (1979) Distortions in the tetrahedral oxyanions of crystalline substances. N Jahrb Mineral Abh 137:54–73

Kobtsev BM, Kharitonov YA, Pobedimskaya EA, Belov NV (1968) Crystal structure of $LiCd[MoO_4]OH$. Sov Phys Doklady 13:193–195

Leavitt RP (1982) On the role of certain rotational invariants in crystal field theory. J Chem Phys 77:1661–1663

Newman DJ (1971) Theory of lanthanide crystal fields. Adv Phys 20:197–256

Newman DJ, Ng B (1989) The superposition model of crystal fields. Rep Prog Phys 52:699–763

Newman DJ, Ng B (2000) Crystal field handbook. Cambridge University Press, Cambridge

Renner B, Lehmann G (1986) Correlation of angular and bond length distortions in TO_4 units in crystals. Z Krist 175:43–59

Rentzeperis PJ (1963) The crystal structure of hodgkinsonite $Zn_2Mn[(OH)_2|SiO_4]$. Z Krist 119:117–138

Reshak AH, Khan W (2014) Electronic structure, optical and thermoelectric transport properties of layered polyanionic hydrosulfate $LiFeSO_4OH$: Electrode for Li-ion batteries. J Alloys Comp 591:362–369

Robinson K, Gibbs GV, Ribbe PH (1971) Quadratic elongation: a quantitative measure of distortion in coordination polyhedra. Science 172:567–570

Rudowicz C, Gnutek P, Açikgöz M (2019) Superposition Model in electron magnetic resonance spectroscopy – a primer for experimentalists with illustrative applications and literature database. Applied Spectr Rev 54:673–718

Rudowicz C, Gnutek P, Karbowiak M (2011) Forms of crystal field Hamiltonians - a critical review. Opt Mater 33:1557–1561

Rudowicz C, Jian Q (2002) The extended version of the computer package CST for conversions, standardization and transformations of the spin Hamiltonian and the crystal-field Hamiltonian. Comp Chem 26:149–157

Rudowicz C, Yeung YY, Du ML, Chang YM (1992) Manual for the crystal [ligand] field computer package with appendix: Tables of values of the parameters B, C, and ξ for $3d^4$ and $3d^6$ free ions and ions in crystals. Research Report, Department of Applied Science, City Polytechnic of Hong Kong, Hong Kong, 45pp

Sheldrick GM (2008) A short history of SHELX. Acta Cryst A64:112–122

Sheldrick GM (2015) Crystal structure refinement with *SHELXL*. Acta Cryst C71:3–8

Subban CV, Ati M, Rousse G, Abakumov AM, Van Tendeloo G, Janot R, Tarascon J-M (2013) Preparation, structure, and electrochemistry of layered polyanionic hydroxysulfates: LiMSO4OH (M = Fe Co, Mn) electrodes for Li-ion batteries. J Am Chem Soc 135:3653–3661

Wenger M, Armbruster T (1991) Crystal chemistry of lithium: oxygen coordination and bonding. Eur J Min 3:387–399

Wildner M (1992) On the geometry of $Co(II)O_6$ polyhedra in inorganic compounds. Z Krist 202:51–70

Wildner M, Andrut M, Rudowicz CZ (2004) Optical absorption spectroscopy in geosciences. Part I: Basic concepts of crystal field theory. EMU Notes in Mineralogy 6:93–143

Wildner M, Beran A, Koller F (2013b) Spectroscopic characterisation and crystal field calculations of varicoloured kyanites from Loliondo, Tanzania. Mineral Petrol 107:289–310

Wildner M, Büchel GE, Filak L, Petautschnig C, Giester G (2013a) Crystal structure, polarised optical absorption spectra, and crystal field Superposition Model analysis of the new compound $LiCo(SO_4)OH$. Z Krist Suppl Issue 33:93–94

Yang ZY, Hao Y, Rudowicz C, Yeung YY (2004) Theoretical investigations of the microscopic spin Hamiltonian parameters including the spin–spin and spin–other-orbit interactions for $Ni^{2+}(3d^8)$ ions in trigonal crystal fields. J Phys Cond Mat 16:3481–3494